Metabolomics
DOI 10.1007/s11306-014-0660-z

ORIGINAL ARTICLE

A non-targeted metabolomics approach to evaluate the effects of biomass growth and chitosan elicitation on primary and secondary metabolism of *Hypericum perforatum* in vitro roots

Elisa Brasili · Giulia Praticò · Federico Marini · Alessio Valletta · Giorgio Capuani · Fabio Sciubba · Alfredo Miccheli · Gabriella Pasqua

Received: 9 January 2014 / Accepted: 2 April 2014

Abstract *Hypericum perforatum* L. is a medicinal plant commonly used worldwide for the treatment of mild and moderate depression due to its wide range of bioactive compounds. *H. perforatum* regenerated roots have been proposed as an efficacious in vitro system to biosynthesize pharmaceutically useful secondary metabolites. In the present study, a metabolomic platform, which integrates an nuclear magnetic resonance (NMR)-based metabolic profiling and analysis of variance-simultaneous component analysis (ASCA), has been applied in order to characterize the changes of the primary and secondary metabolism of *H. perforatum* regenerated roots induced by an achieved high biomass density in a confined growth environment or in response to chitosan treatment.The ASCA modelling applied to NMR-based metabolic profiling allowed to recognize the effects due to biomass growth rate changes and chitosan treatment. With an high biomass density, associated to a decelerating biomass growth rate, the levels of tryptophan, fructose, shikimic acid, and epicatechin increased, whereas γ-aminobutyric acid and histidine decreased. In response to chitosan elicitation, the biomass growth was arrested and valine, isoleucine, glutamine, γ-aminobutyric acid, fructose, sucrose, polyunsaturated fatty acids, epicatechin, xanthones, dimethylallyl-pyrophosphate, and stigmasterol levels increased, while histidine levels decreased. The metabolic profiling of regenerated roots shows how the cultures respond to different stress conditions: production of epicatechin in response to high biomass density and production of epicatechin, xanthones and isoprenoids in response to chitosan-treatment. This approach can be applied to define suitable protocols to produce the desired secondary metabolites with different bioactivities.

Keywords *Hypericum perforatum* in vitro roots · Metabolic profiling · Metabolomics · ASCA modelling · NMR spectroscopy

1 Introduction

Hypericum perforatum (common St. John's wort) is a perennial herb which is distributed globally (except Antarctica) (Nürk et al. 2013) and is commonly used worldwide for the treatment of mild and moderate depression (Butterweck 2003; Crockett and Robson 2011; Nahrstedt and Butterweck 2010). Research on St. John's wort has been focused primarily on hypericins and hyperforins as the major constituents of the aerial parts of the plant and responsible for the antidepressant activity (Walker et al. 2002). *H. perforatum* plant extracts also show a broad range of other pharmacological activities, including anticancer, anti-inflammatory, antiviral, antioxidant, and antibacterial properties (Birt et al. 2009; Saddiqe et al. 2010; Caraci et al. 2011) that may be correlated to other bioactive compounds. Although much is known about the medicinal properties of the aerial parts, little is known about the chemical composition or the potential applications of the

Electronic supplementary material The online version of this article (doi:10.1007/s11306-014-0660-z) contains supplementary material, which is available to authorized users.

E. Brasili · A. Valletta · G. Pasqua
Department of Environmental Biology, "Sapienza" University of Rome, P. le Aldo Moro 5, 00185 Rome, Italy

G. Praticò · F. Marini · G. Capuani · F. Sciubba · A. Miccheli (✉)
Department of Chemistry, "Sapienza" University of Rome, P. le Aldo Moro 5, 00185 Rome, Italy
e-mail: alfredo.miccheli@uniroma1.it

Published online: 12 April 2014

H. perforatum root extracts (Tocci et al. 2013; Crockett et al. 2011).

Roots of many species have been studied because of the presence of high value bioactive molecules (Baque et al. 2012; Paek et al. 2009) but the composition of products obtained from wild-grown plants can be greatly affected by several environmental biotic and abiotic factors and the content of bioactive secondary metabolites can be variable and not always satisfactory for application purposes. Since the production of biomass and metabolites is significantly affected by various parameters that need to be optimized, plant cell, tissue and organ cultures are considered effective systems to produce natural products for bioprocessing applications (Rao et al. 2002; Pasqua et al. 2003; Ferrari et al. 2005; Zhang et al. 2013). It has been demonstrated that *H. perforatum* root cultures, because of their high rate of proliferation and high genetic and metabolic stability, are an efficacious alternative system for controlling the factors that affect metabolic pathways and for biosynthesizing phytochemical compounds (Cui et al. 2010, 2011; Zobayed et al. 2004).

Chitosan is frequently used as an elicitor to stimulate the production of pharmaceutically useful compounds both in *in planta* and in in vitro systems (Yin et al. 2012). Chitosan elicitation has been also adopted as an effective strategy to enhance secondary metabolite production, such as xanthones and other polyphenols, in *H. perforatum* in vitro roots (Tocci et al. 2012, 2013) but up to date how the chitosan affects the root metabolome has not been studied.

An analytical technique employed to study the metabolome and to obtain a large quantity of data is nuclear magnetic resonance (NMR) spectroscopy. In non-targeted metabolomic analysis, NMR spectroscopy has afforded some important advantages that can be summarized as ease of quantification, reproducibility, straightforward metabolite identification and its ability to determine unexpected metabolites (Kim et al. 2011). NMR based metabolomic has been applied in quality controls for medicinal plants (Rasmussen et al. 2006; Agnolet et al. 2010; Yang et al. 2006; Falasca et al. 2013), in chemotaxonomy studies (Kim et al. 2010; Matsuda et al. 2010), in the study of the biological activity of plant preparations (Modarai et al. 2010) of plant interactions with other organisms (Jahangir et al. 2008) of the fruit ripening process (Capitani et al. 2010) and of genetically transformed plants (Manetti et al. 2006). Finally, NMR-based metabolomic analysis has been applied to investigate the interplay between primary and secondary metabolism in Opium poppy cells treated with a fungal elicitor (Zulak et al. 2008). Recently, NMR fingerprinting was used to investigate the natural product diversity within the genus *Hypericum* and its correlation to bioactivity, exemplified by cytotoxic properties (Porzel et al. 2013).

The aim of the present study was to characterize the changes in the primary and secondary metabolism of in vitro regenerated roots of *H. perforatum* subsp. *angustifolium* during growth in a confined culture environment and in response to chitosan elicitation. A metabolomic platform integrating non-targeted NMR-based metabolic profiling and multivariate analysis such as ANOVA-simultaneous component analysis (ASCA) was used.

2 Materials and methods

2.1 Plant material and root cultures

In vitro regenerated roots of *H. perforatum* were obtained according to the procedures described by Tocci et al. (2011).

Liquid root cultures were established after 30 days by inoculating 1 g fresh weight (FW) of roots in magenta vessels containing 80 ml liquid MS medium supplemented with glucose (2.2 g l^{-1}) and IBA (1 mg l^{-1}). The magenta vessels were shaken at 100 rpm at 25 ± 1 °C and maintained in the continuous darkness. Since optimum nutrient concentration is a critical point in controlling growth of regenerated roots and accumulation of secondary metabolites (Lian et al. 2002), the medium was renewed every 4 days, the time necessary for biomass duplication. The roots were elicited using chitosan (medium molecular weight; Sigma-Aldrich, Milan, Italy) dissolved in water acidified with HCl (1 M) up to a final concentration of 200 mg l^{-1} which was added on the twelfth day of culture using a 0.22 μm sterile filter (Tocci et al. 2011). An appropriate amount of water was added to the control samples. The growth curve of root biomass was recorded during a period of 15 days from inoculum. Regenerated roots were harvested at day twelve (time 0), day thirteen (24 h, time 1) and day fifteen (72 h, time 2) and divided into five groups: basal (time 0), control and treated to 24 h after elicitation (time 1) and control and treated to 72 h after elicitation (time 2).

2.2 NMR sample preparation

The metabolic quenching of the roots was performed by rapidly freezing in liquid N_2. The frozen biomass (1.5 g) was ground up in a steel pestle in liquid N_2 and extracted by a solvent mixture of methanol, chloroform and distilled water at 2:2:1.2 (v/v ratio), according to the modified Bligh-Dyer procedure for plant samples (Miccheli et al. 1988; Manetti et al. 2004). 4.5 ml CH_3OH:$CHCl_3$ (2:1 v/v ratio) mixture was added to the frozen powder and after mixing 1.5 ml $CHCl_3$ and 1.8 ml H_2O were added. The samples were mixed by vortex for 1 min and allowed to

stand overnight at 4 °C then centrifuged for 30 min at 11,000×*g* at 4 °C. The resulting upper hydro-alcoholic and lower organic phases were then carefully separated and dried under N_2 flow. The dried phases were stored at −80 °C until the NMR analysis.

2.3 NMR spectroscopy

The dried residue of the hydro-alcoholic phase was dissolved in 0.6 ml CD_3OD/D_2O (1:2 v/v ratio) containing 3-(trimethylsilyl)- propionic-2,2,3,3,-d_4 acid sodium salt (TSP, 2 mM) as internal standard (chemical shift reference). The dried residue of the chloroformic phase was dissolved in 0.6 ml $CDCl_3$, (Cambridge Isotope Laboratories, Inc.), (99.8 %) containing 1,1,3,3,5,5-hexamethylcyclo-tri-siloxane (HMS) (Sigma-Aldrich, Usa) as internal standard (2 mM). NMR spectra were obtained using a Bruker Avance 400 spectrometer operating at a frequency of 400.13 MHz for the proton. One dimensional proton spectra were acquired at a temperature of 298 K with a spectral width of 15 ppm, 64 k data points, 128 scans with an acquisition time of 5.45 s and a relaxation delay of 5.05 s for a total repetition time of 10.5 s complying with the full relaxation condition after a 90 degree pulse.

The univocal assignation of proton resonances was achieved by means of bidimensional ^{1}H homonuclear total correlation spectrosopy (TOCSY) experiments and by bidimensional ^{1}H-^{13}C heteronuclear single quantum coherence (HSQC) experiments.

Homonuclear experiments were recorded at 298 K with a spectral width of 15 ppm in both dimensions employing a matrix of 2k × 512 data points, a repetition time of 2 s and 64 scans. The mixing time for the ^{1}H-^{1}H TOCSY was 110 ms. HSQC experiments were acquired with a spectral width of 15 ppm in proton dimension and 220 ppm in the carbon one, employing a matrix of 2k × 256 data points for the proton and the carbon dimensions, respectively, a repetition delay of 2 s and 128 scans. The water signal was suppressed using solvent pre-saturation, with the irradiation time following the relaxation delay. In order to minimize the variability of signal intensity due to water suppression, a careful calibration of the soft pulse for water suppression was always performed.

1D-NMR spectra were processed using 1D-NMR Manager ver. 12.0 software (Advanced Chemistry Development, Inc., Toronto, Ontario, Canada), whereas 2D-NMR spectra were processed using Bruker Top Spin (Bruker, Karlsruhe, Germany).

2.4 Multivariate analysis

Multivariate data analysis was carried out using in house-written functions operating under Matlab R2012b environment (The MathWorks, Inc., Natick, MA, USA). Spectral data were mean-centered and scaled before analysis. Principal components analysis (PCA) was used to investigate inherent clustering and to identify outliers. In order to assess whether treatment and/or time (corresponding to biomass density) had an effect on the metabolic profiles, as determined by NMR spectroscopy, ANOVA-simultaneous component analysis (ASCA) (Smilde et al. 2005; Jansen et al. 2005) was used. ASCA can be considered as an extension of the ANOVA to multivariate data and is particularly useful when the significance of the effect of one or more factors on the experimental data can be evaluated (Vis et al. 2007). ASCA operates by partitioning the variation of the experimental data, collected by NMR spectra, of different samples into the contributions induced by the effect of controlled factors, usually a treatment or an experimental condition, or of their interactions, and by analyzing the resulting matrices by simultaneous component analysis (SCA), a method similar to PCA (Kiers et al. 1994). Accordingly, the mean-centered matrix $\mathbf{X}_c$ of the experimental data is partitioned into the individual matrices accounting for the effects of time, treatment, time-treatment interaction, and for the residual variation (associated to the experimental error):

$$\begin{aligned}\mathbf{X}_c &= \mathbf{X} - \mathbf{X}_{mean} \\ &= \mathbf{X}_{treatment} + \mathbf{X}_{time} + \mathbf{X}_{time\times treatment} + \mathbf{X}_{residual}\end{aligned} \quad (1)$$

where $\mathbf{X}_{mean}$ is a matrix the rows of which are all identical to the overall mean profile.

In order to obtain a balanced design, only the data collected at time 24 and 72 h were considered for analysis, which was then carried out on a data matrix comprising 20 observations, i.e. five replicates for each of the 4 time/treatment combinations (control 24 h; control 72 h; treated 24 h; treated 72 h).

Operationally the computation of each of the matrices corresponding to the main effects was carried out as follows. For each of the factors considered, the rows of the centred matrix $\mathbf{X}_c$ corresponding to the different levels of the design were found and averaged, and these calculated mean values were used to build the matrix associated with the effect: if the ith sample corresponds to the 1st level of factor A, the ith row of the matrix $\mathbf{X}_A$ will contain the average vector calculated on all samples for which factor A is at level 1, and so on. Computation of the interaction matrix is carried out similarly, after deflation (=subtraction) of the matrices corresponding to the main effects (Figure S1).

Simultaneous component analysis is then performed on the individual matrices to model the variability corresponding to each effect. From a purely mathematical standpoint, SCA is identical to PCA: the difference is only

philosophical in nature. Indeed, in SCA different samples are modelled at the same time. Accordingly, each of the matrices resulting from the ANOVA partitioning is decomposed as:

$$\mathbf{X}_i = \mathbf{T}_i\mathbf{P}_i^T + \mathbf{E}_i \quad (2)$$

where $\mathbf{T}_i$ and $\mathbf{P}_i$ are the scores and loadings for the ith partition, respectively, and $\mathbf{E}_i$ is the corresponding residual matrix.

It must be stressed that for mean centred two level balanced design like the one in this study, all the partitions corresponding to main effects and interactions are rank one, resulting in zero errors.

As previously described, ASCA partitions the variation of the original matrix into the contribution of the main effects of the controlled factors, of their interactions and residuals. The extent of each contribution is expressed in the form of the sum of squares of the elements of the matrix corresponding to the effect:

$$SSQ_k = \|\mathbf{X}_k\| = \sum_i \sum_j \left(x_{ij}^k\right)^2 \quad (3)$$

where x_{ij}^k is the ith row, jth column entry of the matrix $\mathbf{X}_k$. In order to assess whether an effect is significant or not, the experimental sum of squares has to be compared with the distribution of values corresponding to the null hypothesis. In this study, for each factor and interaction, the distribution of the values of the sum of squares corresponding to the null hypothesis (no significance of the considered effect) was estimated non parametrically by means of a permutation (randomization) test. The permutation test works by uncoupling the group labels from the data and randomly reassigning them: it does not change the metabolite value for a sample, but just reassigns the sample randomly to one of the treatment groups. Partitioning the permuted data according to the ANOVA scheme and computing the corresponding sum of squares.

$$SSQ_k^{perm} = \left\|\mathbf{X}_k^{perm}\right\| = \sum_i \sum_j \left(x_{ij}^{k,perm}\right)^2 \quad (4)$$

allows it to be checked whether the results with randomized data are as different from zero as those obtained from the experimental data. Repeating the randomization procedure for an appropriate number of times, each time calculating the corresponding sum of squares, provides an empirical distribution of the SSQ_k values for the null hypothesis. Validation of the significance of the effect is then carried out by comparison of the SSQ_k obtained from the experimental data with this distribution (Vis et al. 2007).

The total variation of the experimental matrix was then partitioned according to Eq. 1 and the significance of the main effects (time and/or elicitation) and of their interaction was evaluated by permutation test (Vis et al. 2007).

Simultaneous component analysis (after Pareto scaling) was used to model the variation in the two corresponding matrices $\mathbf{X}_{treatment}$ and $\mathbf{X}_{time}$. As only two levels were considered for each factor, single component models explained 100 % of the variance of the individual matrices, i.e. each matrix $\mathbf{X}_i$ was decomposed into the product of one score and one loading vector.

In order to use SCA results for the interpretation of the metabolic effect of the considered factors, the significance of the contribution of the experimental variables to the definition of the models (i.e. the significance of the loadings) had to be assessed: if the loading of a variable is statistically different from zero, then the factor has an effect on the concentration of that metabolite. In particular, a bootstrap procedure was used to calculate the empirical distribution of the loadings, so as to be able to check their significance. Operationally, at each bootstrap cycle, a new partition $\mathbf{X}_i^{bstp}$ was constructed from the mean centered matrix by including, for each level, a random subset of the original samples with repetitions, taking care that the numerosity of each treatment group was preserved. For instance, if the effect considered has two levels and, in the original matrix, samples 1–10 correspond to level 1 and samples 11–20 correspond to level 2, one bootstrap cycle could produce a matrix made up of samples [1 2 2 2 5 5 6 7 9 10 12 13 13 14 16 16 16 18 19 19]. ASCA analysis on this matrix will result in an estimate of the loading vector for the effect so that repetition of the procedure for a significant number of times (in our study 100000) will produce an empirical distribution of the values of the loadings for each variable. A metabolite is then considered to contribute significantly to the model if, based on this distribution, its loading is statistically different from zero.

3 Results and discussion

3.1 Effects of biomass growth on primary and secondary metabolism

The growth curve of both chitosan and non- treated *H. perforatum* in vitro roots is shown in Fig. 1. In chitosan treated roots, the chitosan addition at day 12 caused a sudden slowdown of growth, whereas the growth of the control roots continued. The inhibitory effect of chitosan on biomass growth in root cultures has been also reported for other species such as *Ocimum basilicum* L. (Bais et al. 2002) and *Withania sominifera* (L.) Dunal (Sivanandhan et al. 2012).

The hydroalcoholic and chloroformic total extracts obtained from chitosan-treated and control roots were

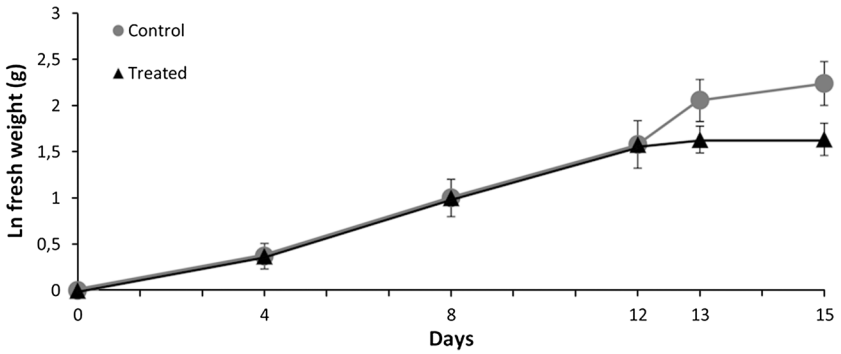

Fig. 1 The growth curve of *H. perforatum* in vitro roots over a period of 15 days. Growth is expressed as a natural logarithm of fresh weight biomass. Chitosan solution or the respective volume of water was added at day 12 for elicitor-treated or non-treated roots, respectively. Data are presented as the mean ± standard deviation (SD) of five biological repeats

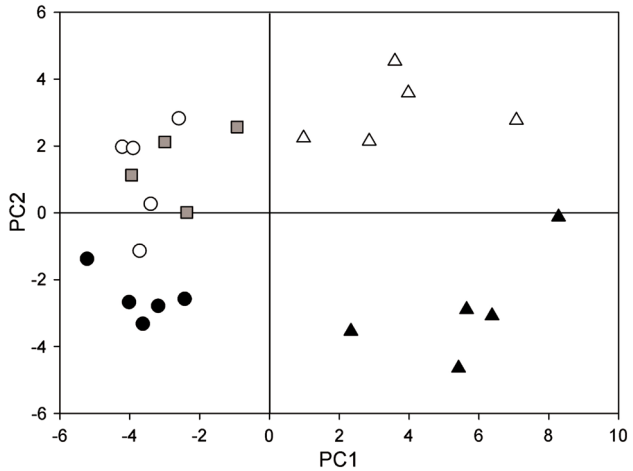

Fig. 2 The PC scores plot relative to whole set of *H. perforatum* root data. *Open square* basal samples; *open circle* non-treated samples at 24 h, *filled circle* non-treated samples at 72 h; *open triangle* chitosan-treated samples at 24 h; *filled triangle* chitosan-treated samples at 72 h. Total variance explained by PCs was 40 and 15.4 % for PC1 and PC2, respectively

investigated by ^{1}H-NMR spectroscopy and sixty-four metabolites were assigned (Table S1). The concentrations of forty-seven metabolites measured at basal time, 24 and 72 h both in the control and the chitosan-treated roots are reported in Figures S2-S5.

Several changes of primary and secondary metabolites, including levels of amino acids, carbohydrates, small organic acids, lipids, phenolics, isoprenoids, and other compounds related to plant metabolism were observed. An initial exploration of the whole data set was performed by principal component analysis (PCA) on the concentration of metabolites, measured at basal time (day 0), 24 and 72 h after elicitation. The PCA score plot shows that root samples were clustered on the basis of PC1 and PC2 scores corresponding to chitosan elicitation and to biomass growth-related changes, respectively (Fig. 2). However, the PC2 scores did not allow a separation between basal and 24 h root samples.

Analysis of variance-simultaneous component analysis modelling was applied in order to determine the metabolic variations related to root biomass growth and to chitosan treatment, and to the interaction between them. A balanced experimental design was constructed considering only the data at time 24 and 72 h, excluding the basal samples.

Analysis of variance-simultaneous component analysis modelling showed that chitosan treatment and biomass increase respectively accounted for 24.1 and 23.5 % of the variation in the original mean-centred matrix, while their interaction explained 3.7 % of the variance. The randomization test with 100,000 permutations showed that only the effects of chitosan treatment and biomass increase were significant with P values 0.0048 and 0.0053, respectively, while the effect of their interaction was not statistically different from zero ($P = 0.2493$) (Fig. 3a, b).

Having verified that elicitation and biomass increase had a significant effect on the metabolic profiles of *H. perforatum* roots, simultaneous component analysis (SCA) was used (after Pareto scaling) to model the variation in the two corresponding matrices $\mathbf{X}_{elicitation}$ and $\mathbf{X}_{time}$. The distribution of the loadings for the SCA models of the two main effects is reported in Fig. 3c, d. In Fig. 3e, the loadings of the significant metabolites for either the time or the treatment models are displayed by a heatmap. This figure allows a rapid identification of the metabolites significant for the time and the treatment models; the colours define the versus of changes (blue/decrease, red/increase and white/not significant changes).

The results of ASCA modelling, associated with the data of root growth curve, enable the "time effect" to be mainly defined as the effect of the increase of biomass density in a confined environment. Control roots showed an increase in flavonoid levels, such as epicatechin, and shikimate

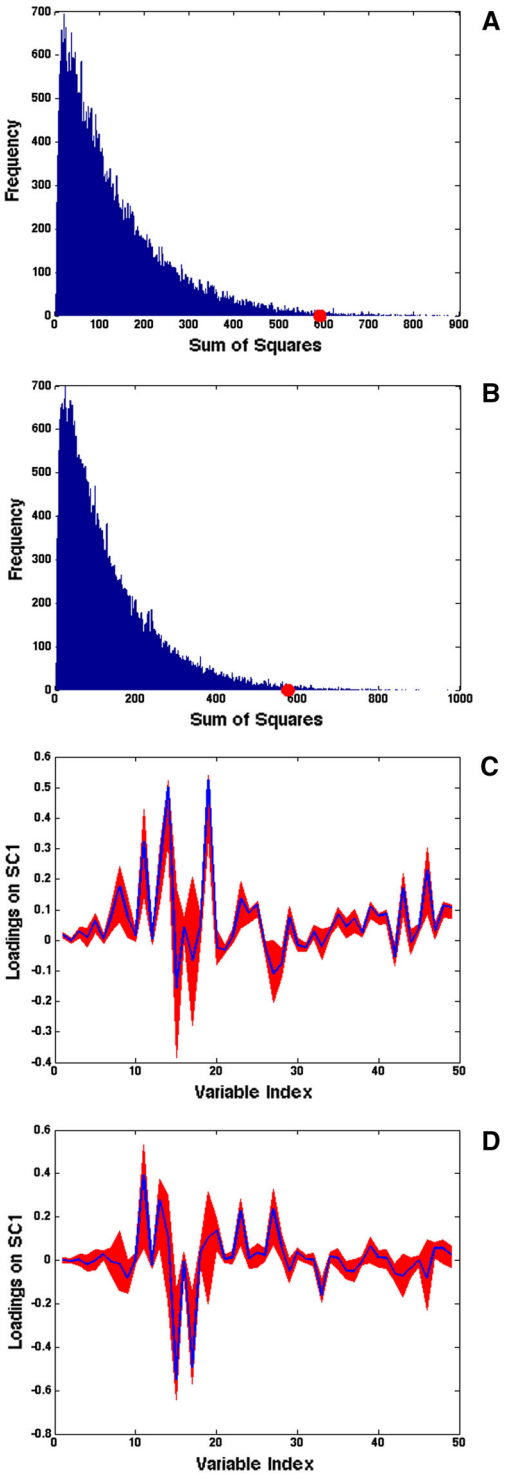

E

Loadings number	Metabolites	Time	Treatment
1	U1		
3	Isoleucine		
5	Valine		
6	U3		
7	Lactate + threonine		
8	Alanine		
9	GABA		
11	Glutamine		
13	Fructose		
14	Sucrose (fructose)		
15	α -Glucose		
16	U4		
17	β -Glucose		
18	U5		
19	Sucrose (glucose)		
20	U6		
21	U7		
23	Epicatechin		
24	U8		
25	U9		
26	U10		
27	Shikimate		
28	U11		
29	U12		
30	Tryptophan		
31	U13		
32	Adenosine		
33	Formate		
34	Trigonelline		
35	DMAPP		
36	U14		
37	U15		
38	U16		
39	U17		
40	U18		
41	U19		
42	Histidine		
43	Benzoyl moiety		
45	Stigmasterol		
46	PUFA		
47	Xanthone		
48	Total xanthones		
49	Other xanthones		

Fig. 3 ASCA modelling. Evaluation of the significance of the multivariate effect of elicitation (**a**), and time (**b**) by means of permutation tests. The *blue histograms* represent the distributions of sum of squares values under the null hypothesis, while the *red dots* correspond to the experimentally observed values. SCA analysis on the effect matrices for elicitation (**c**) and time (**d**): variable loadings for the one-component SCA model (*blue line*) and their 95 % confidence intervals (*red*). **e** Heatmap highlighting the metabolites that contribute significantly to the model for time and elicitation effects. *Red* corresponds to significant loadings with positive sign (increase); *blue* corresponds to significant loading with negative sign (decrease); *white* indicates metabolites whose loadings were not significant (Color figure online)

pathway intermediates, such as shikimic acid, associated with an increase in biomass density and with a decrease in growth rate between day 13 and 15.

The relationship between biomass density, the slow-down in biomass growth and phenol biosynthesis was also observed by Cui et al. (2010) in *H. perforatum* roots cultured in bioreactor. In the control roots a significant correlation between tryptophan (Trp) and epicatechin increased levels ($r = 0.78$, Pearson's correlation) was observed and this result pointed to a stimulation of the phenylpropanoid pathway caused by a higher root biomass density in a confined environment.

Regarding the metabolism of aminoacids, opposite trends were observed in γ-aminobutyric acid (GABA), histidine, and glutamine. In particular, a decrease in GABA and histidine and an increase in glutamine occurred with increasing culture time. Moreover, a slight increase in fructose and no significant changes in sucrose levels were observed. It is a known fact that the slower growing plants invest more of their total root metabolites in carbon- and nitrogen-storage compounds (Atkinson et al. 2012). In our results the slight increase in glutamine, which plays a role in nitrogen storage, could be explained by a decelerating growth. Indeed, the increase in glutamine levels was ever more significant in elicitor-treated roots, when a biomass growth arrest occurred.

In control roots, fructose levels correlated significantly with shikimate ($r = 0.89$) and with xanthones ($r = 0.72$), but correlated inversely with histidine ($r = -0.77$). This correlation pattern seems to illustrate the biochemical relationship between the synthesis of fructose, through transaldolase or transketolase, and histidine synthesis, starting from other intermediates in the pentose phosphate pathway. A competition between metabolic fluxes involving pentose phosphate pathway intermediates towards fructose/erythrose-4-phosphate (via transketolase and transaldolase reactions), channelled through the biosynthesis of shikimate and phenylpropanoid metabolites and histidine biosynthesis (via oxidative penthose phosphate pathway and isomerase reactions), could be hypothesized.

The increase in glutamine levels associated with a decrease in GABA levels ($r = -0.72$) is of interest. GABA is a ubiquitous non-protein amino acid that in plants has been linked to stress, signalling and storage (Fait et al. 2008). It has long been known that GABA is derived from glutamate, through glutamate decarboxylase (GAD) activity, and is then converted to succinic semialdehyde and succinate, which enters the tricarboxylic acid cycle. GAD activity is confined to the cytosol, specific for glutamate, and regulated by pH and Ca^{2+}-calmodulin (Shelp et al. 1999). It has been reported that this proton-consuming reaction can limit cytosolic acidosis in certain species during exposure to various stress conditions such as hypoxia (Shelp et al. 1999). The relationship observed between time-related decrease in GABA and increase in glutamine suggests a metabolic flux shift from GABA synthesis towards glutamine synthesis, as effect of the increased nitrogen storage due to a lower demand caused by slowdown in biomass growth.

3.2 Effects of chitosan elicitation on primary and secondary metabolism

In the chitosan-treated roots ASCA results (Fig. 3) showed a significant increase in sucrose and fructose but not in glucose levels at 24 and 72 h after elicitation. A significant increase in aminoacid levels, such as isoleucine, valine, glutamine, GABA, alanine, were observed together with a decrease in histidine.

The observed metabolic profile of root extracts is consistent with slowdown or arrested growth, which causes a metabolic shift towards a storage of carbon and nitrogen compounds, such as sucrose and aminoacids (Atkinson et al. 2012). However, this metabolic profile reflects also a process of adaptation to stress conditions induced by chitosan treatment.

Since it is well known that the early defence responses elicited by chitosan include a raising of cytosolic H^+ and Ca^{2+} concentrations (Zhao et al. 2005), the observed levels of GABA that are higher than control roots, in particular at 24 h after the chitosan treatment, can be related to a higher GAD activity stimulated by an altered intracellular H^+ and Ca^{2+} homeostasis (Kinnersley and Turano 2000; Snedden et al. 1995).

An increase in phenylpropanoid-derived secondary metabolites in chitosan-treated roots was displayed by the ASCA model. In particular, epicatechin and xanthone levels were two- and eight-fold higher, respectively, than the corresponding control samples at 72 h after elicitation (Figures S2-S5). Xanthones and flavonoids are synthesized from phenylalanine through shikimate pathway.

In chitosan-treated roots, the level of shikimate was lower than in control roots, while benzoyl-moiety levels were ten-fold higher. Our results indicate that both the phenylpropanoid and xanthone pathways were specifically stimulated by chitosan treatment, and they are in agreement with previous results obtained by Tocci et al. (2011), which observed an accumulation of xanthones using the same experimental system. A scheme of the above metabolic pathways is reported in Fig. 4.

Chitosan has been extensively studied with regard to its effects on enzymes involved in the phenylpropanoid pathway (Baque et al. 2012; Chakraborty et al. 2009). Chitosan mimics a fungal infection, inducing a non-host resistance through PRR-mediated recognition and priming a systemic acquired immunity (Iriti and Faoro 2009). The observed increase in xanthones supports the hypothesis proposed by Franklin et al. (Franklin et al. 2009) that these metabolites act as phytoalexines, playing a role in plant chemical defence against pathogen attack.

Also of interest is the increase in dimethylallyl-pyrophosphate (DMAPP) observed in chitosan elicitor-treated roots of *H. perforatum*. DMAPP content in treated roots was seven-fold higher at 24 h and ninefold higher at 72 h than their respective controls. DMAPP, together with its isomer isopentenyl pyrophosphate (IPP), is the precursor of the isoprenoid compounds, including molecules such as sterols, dolichols, triterpenes, ubiquinone, components of

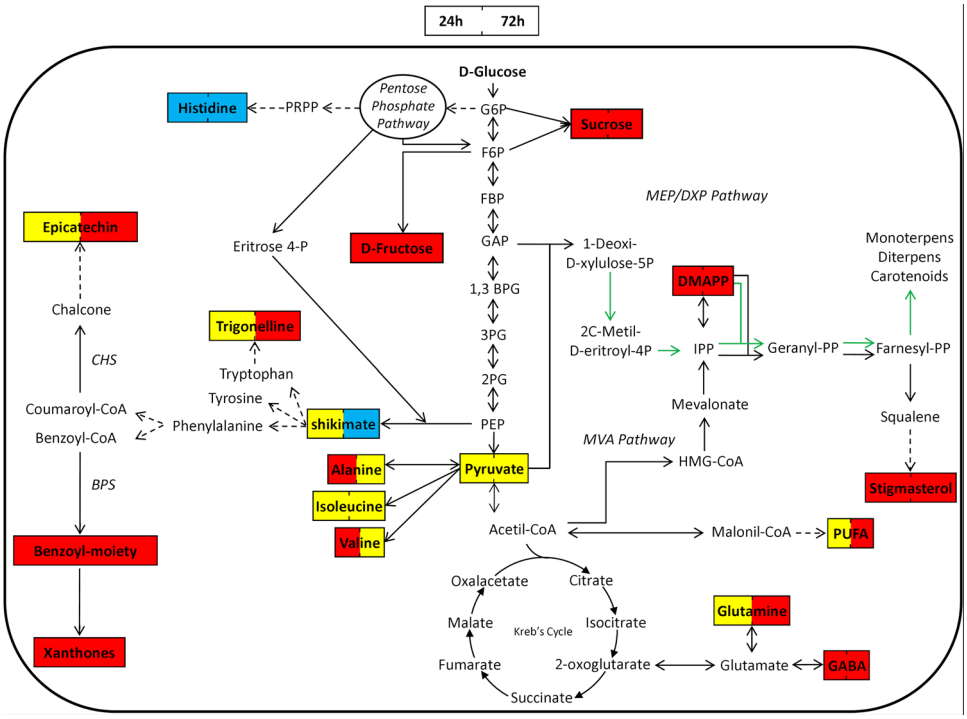

Fig. 4 Schematic representation of root metabolic network. The metabolite level changes observed after 24 and 72 h of chitosan elicitation are shown. The significant metabolites as evaluated by ASCA modelling for chitosan treatment effect are represented by *coloured boxes*. The *colour code* designates changed and unchanged metabolite abundances as follows: *red*—significantly increased; *yellow*—not significantly changed; *blue*—significantly decreased. The significant differences between treated and control at corresponding experimental times were further assessed by using Student's *t* test. *Solid arrows* in the network diagram specify a single step connecting two metabolites; *dashed arrows* indicate at least two steps. *CHS* chalcone synthase, *BPS* benzophenone synthase (Color figure online)

macromolecules such as prenyl groups, and isopentenylated tRNAs (Sacchettini and Poulter 1997; Kuzuyama and Seto 2003). Although DMAPP could be considered as a substrate also for the synthesis of isoprenylated xanthones, we have not found any significant linear correlation between DMAPP and xanthones levels (Pearson's coefficient $r = 0.014$) in chitosan-treated roots, whereas a significant negative correlation between DMAPP and sitosterols ($r = -0.59$) was found, suggesting a biochemical relation between intermediate and product.

The diversity of isoprenoids reflects the variety of important biological functions, including electron transport in respiration and photosynthesis, hormone-based signalling, the regulation of transcriptional and post-translational processes that control lipid glycoprotein biosynthesis, protein cleavage degradation, meiosis and apoptosis. The isoprenoids are also important structural components of cell and organelle membranes (Hunter 2007, 2011). In addition, they can play a crucial role as phytoalexins, because many of them exert antibiotic, antiviral and fungitoxic or fungistatic activities (Ahuja et al. 2012). An increase in concentration of the isoprenoid phytoalexins in response to fungal elicitors in the roots has been also observed in *Oryza sativa* L., in which fungal chitin oligosaccharide stimulated the roots to biosynthesize and release several diterpenoids into the medium (Toyomasu et al. 2008).

Dimethylallyl-pyrophosphate and isopentenyl pyrophosphate may be produced through two independent metabolic pathways: the acetate-mevalonate (MVA) pathway and the non-mevalonate pathway (non-MVA), also called the 1-deoxy-D-xylulose-5-phosphate (DXP) or the 2-C-methyl-D-erythritol-4-phosphate (MEP) pathway (Hunter 2007). In plants, the MVA and non-MVA pathways are compartmentalized in the cytoplasm and plastid, respectively. Sesquiterpenes, sterols, and polyterpenes are derived via the cytosolic MVA pathway, whereas isoprene, phytol, carotenoids, and the plant hormones gibberellic and abscisic acid are synthesized via the plastid non-MVA pathway (Hsieh and Goodman 2005).

^{1}H-NMR analysis failed to reveal the presence of terpenoids. However, mono- and sesquiterpenes were isolated in *Hypericum perforatum* L. roots by GC–MS (Motavalizadehkakhky 2012).

It is interesting that high stigmasterol levels have been found in chitosan-treated roots. Stigmasterol is synthesized inside the cytosol through the cytochrome P450 CYP710A1 via C22 desaturation from β-sitosterol originating from

reactions involved in the sterol branch of the isoprenoid pathway (Benveniste 2004). Despite an increased synthesis of stigmasterol, the results show that β-sitosterol levels were found to remain constant at 24 h and 72 h after chitosan treatment, indicating that the chitosan treatment stimulated the *de novo* synthesis of β-sitosterol and its desaturation through the sterol biosynthetic pathway.

An increased synthesis of stigmasterol was found in different plant-pathogen interactions. The conversion of β-sitosterol to stigmasterol in *Arabidopsis thaliana* leaves was observed 10 and 48 h after inoculation of virulent and avirulent *Pseudomonas syringae* strains (Griebel and Zeier 2010). These authors found that the pathogen-stimulated stigmasterol was triggered by the perception of pathogen-associated molecular patterns (PAMPs) and the generation of reactive oxygen species (ROS) (Griebel and Zeier 2010).The role of stigmasterol in plants during stress is still poorly understood. Sitosterol and stigmasterol, like brassinosteroids, are involved in the regulatory function of plant development, affecting gene expression involved in cell expansion and division, vascular tissue differentiation and several developmental programs (Sasse 2003). Several reports have proposed the existence of sterol-membrane microdomains, so-called lipid rafts, which may play a role in the recruitment of molecular components involved in plant defence signalling (Bhat and Panstruga 2005). In particular, it has been suggested that a pathogen-induced change in stigmasterol/sitosterol ratio can influence different physicochemical properties of membrane microdomains and thereby modulate plant defence signalling (Griebel and Zeier 2010).

Moreover, the increase in polyunsaturated fatty acids observed is in agreement with the results found for *A. thaliana* leaves treated with *P. syringae* (Yaeno et al. 2004).

On the basis of the above evidence, the increases in polyunsaturated fatty acids and in stigmasterol levels suggest a stimulation of a lipid desaturation process that may have altered the membrane microdomains, favouring a change in membrane permeability.

In Fig. 4 the effects of chitosan treatment on primary and secondary metabolism of *H. perforatum* regenerated roots are displayed. The figure summarizes how the metabolic pathways of the regenerated roots respond to chitosan treatment: (1) stimulation of phosphate pentose pathway through a higher trans-ketolase/trans-aldolase activities rather than the PRPP synthesis pathway: this leads to a high production of erithrose-4-phosphate as an intermediate of the shikimate pathway and, therefore of the phenyl-propanoid synthesis; (2) storage of sugars as well as of amino acids (mainly glutamine and GABA) due to their lower utilization for energy production and protein synthesis, respectively; this is consistent with the slowdown or complete arrest of growth; (3) shift of acetyl-CoA utilization from the mitochondrion energetic production to the cytoplasmatic synthesis of lipids such as PUFA and sterols.

Furthermore, a stimulation of the malonyl-CoA synthesis from acetyl-CoA could be requested for its utilization in the flavonoid and xanthone synthesis.

4 Concluding remarks

Non targeted NMR-based metabolic profiling has been used to explore the primary and secondary metabolism of *H. perforatum* regenerated roots. Our approach based on multivariate data analysis, such as ANOVA Simultaneous Component Analysis, has allowed the metabolic effects due to an increase in biomass density to be separated from those due to chitosan elicitation. Moreover, the contemporary stimulation of phenyl-propanoid and isoprenoid pathways with an higher yield of secondary metabolites, such as epicatechin, xanthones and stigmasterols in chitosan-treated roots, in the considered experimental conditions has been observed.

The approach proposed in the present study can be considered an efficient tool for setting up an *H. perforatum* root culture system for large-scale production of specific secondary metabolites useful for pharmacological applications.

Acknowledgments The present study has been supported by a research grant of Sapienza University of Rome 2011—prot. C26A11XLZ5.

Conflict of interest Elisa Brasili, Giulia Praticò, Federico Marini, Alessio Valletta, Giorgio Capuani, Fabio Sciubba, Alfredo Miccheli and Gabriella Pasqua declare that they have no conflict of interest.

References

Agnolet, S., Jaroszewski, J. W., Verpoorte, R., & Staerk, D. (2010). ^{1}H-NMR-based metabolomics combined with HPLC-PDA-MS-SPE-NMR for investigation of standardized *Ginkgo biloba* preparations. *Metabolomics, 6*, 292–302.

Ahuja, I., Kissen, R., & Bones, A. M. (2012). Phytoalexins in defense against pathogens. *Trends in Plant Science, 17*, 73–90.

Atkinson, R. R. L., Burrell, M. M., Osborne, C. P., Rose, K. E., & Rees, M. (2012). A non-targeted metabolomics approach to quantifying differences in root storage between fast- and slow-growing plants. *New Phytologist, 196*, 200–211.

Bais, H. P., Walker, T. S., Schweizer, H. P., & Vivanco, J. M. (2002). Root specific elicitation and antimicrobial activity of rosmarinic acid in hairy root cultures of *Ocimum basilicum*. *Plant Physiology and Biochemistry, 40*, 983–995.

Baque, M. A., Moh, S. H., Lee, E. J., Zhong, J. J., & Paek, K. Y. (2012). Production of biomass and useful compounds from adventitious roots of high-value added medicinal plants using bioreactor. *Biotechnology Advances, 30*, 1255–1267.

Benveniste, P. (2004). Biosynthesis and accumulation of sterols. *Annual Review of Plant Biology, 55*, 429–457.

Bhat, R. A., & Panstruga, R. (2005). Lipid rafts in plants. *Planta, 223*, 5–19.

Birt, D. F., Widrlechner, M. P., Hammer, K. D., Hillwig, M. L., Wei, J., Kraus, G. A., et al. (2009). *Hypericum* in infection: Identification of anti-viral and anti-inflammatory constituents. *Pharmaceutical Biology, 47*, 774–782.

Butterweck, V. (2003). Mechanism of action of St John's wort in depression: What is known? *CNS Drugs, 17*, 539–562.

Capitani, D., Mannina, L., Proietti, N., Sobolev, A. P., Tomassini, A., Miccheli, A., et al. (2010). Monitoring of metabolic profiling and water status of Hayward kiwifruits by nuclear magnetic resonance. *Talanta, 82*, 1826–1838.

Caraci, F., Crupi, R., Drago, F., & Spina, E. (2011). Metabolic drug interactions between antidepressants and anticancer drugs: focus on selective serotonin reuptake inhibitors and *Hypericum* extract. *Current Drug Metabolism, 12*, 570–577.

Chakraborty, M., Karun, A., & Mitra, A. (2009). Accumulation of phenylpropanoid derivatives in chitosan-induced cell suspension culture of *Cocos nucifera*. *Journal of Plant Physiology, 166*, 63–71.

Crockett, S. L., Poller, B., Tabanca, N., Pferschy-Wenzig, E. M., Kunert, O., Wedge, D. E., et al. (2011). Bioactive xanthones from the roots of *Hypericum perforatum* (common St John's wort). *Journal of the Science of Food and Agriculture, 91*, 428–434.

Crockett, S. L., & Robson, N. K. (2011). Taxonomy and chemotaxonomy of the genus *Hypericum*. *Medicinal and Aromatic Plant Science and Biotechnology, 5*, 1–13.

Cui, X. H., Chakrabarty, D., Lee, E. J., & Paek, K. Y. (2010). Production of adventitious roots and secondary metabolites by *Hypericum perforatum* L. in a bioreactor. *Bioresource Technology, 101*, 4708–4716.

Cui, X. H., Murthy, H. N., Jin, Y. X., Yim, Y. H., Kim, J. Y., & Paek, K. Y. (2011). Production of adventitious root biomass and secondary metabolites of *Hypericum perforatum* L. in a balloon type airlift reactor. *Bioresource Technology, 102*, 10072–10079.

Fait, A., Fromm, H., Walter, D., Galili, G., & Fernie, A. R. (2008). Highway or byway: The metabolic role of the GABA shunt in plants. *Trends in Plant Science, 13*, 14–19.

Falasca, A., Melck, D., Paris, D., Saviano, G., Motta, A., & Iorizzi, M. (2013). Seasonal changes in the metabolic fingerprint of *Juniperus communis* L. berry extracts by ^{1}H-NMR-based metabolomics. *Metabolomics*. doi:10.1007/s11306-013-056-1.

Ferrari, F., Pasqua, G., Monacelli, B., Cimino, P., & Botta, B. (2005). Xanthones from calli of *Hypericum perforatum* subsp. *perforatum*. *Natural Product Research, 19*, 171–176.

Franklin, G., Conceição, L. F., Kombrink, E., & Dias, A. C. (2009). Xanthone biosynthesis in *Hypericum perforatum* cells provides antioxidant and antimicrobial protection upon biotic stress. *Phytochemistry, 70*, 60–68.

Griebel, T., & Zeier, J. (2010). A role for beta-sitosterol to stigmasterol conversion in plant-pathogen interactions. *The Plant Journal, 63*, 254–268.

Hsieh, M. H., & Goodman, H. M. (2005). The Arabidopsis IspH homolog is involved in the plastid non mevalonate pathway of isoprenoid biosynthesis. *Plant Physiology, 138*, 641–653.

Hunter, W. N. (2007). The non-mevalonate pathway of isoprenoid precursor biosynthesis. *Journal of Biological Chemistry, 282*, 21573–21577.

Hunter, W. N. (2011). Isoprenoid precursor biosynthesis offers potential targets for drug discovery against diseases caused by apicomplexan parasites. *Current Topics in Medicinal Chemistry, 11*, 2048–2059.

Iriti, M., & Faoro, F. (2009). Chitosan as a MAMP, searching for a PRR. *Plant Signaling and Behavior, 4*, 66–68.

Jahangir, M., Kin, H. K., Choi, Y. H., & Verpoorte, R. (2008). Metabolomic response of *Brassica rapa* submitted to pre-harvest bacterial contamination. *Food Chemistry, 107*, 362–368.

Jansen, J. J., Hoefsloot, H. C., Van der Greef, J., Timmerman, M. E., Westerhuis, J. A., & Smilde, A. K. (2005). ASCA: Analysis of multivariate data obtained from an experimental design. *Journal of Chemometrics, 19*, 469–481.

Kiers, H. A., & ten Berge, J. M. (1994). Hierarchical relations between methods for simultaneous component analysis and a technique for rotation to a simple simultaneous structure. *British Journal of Mathematical and Statistical Psychology, 47*, 109–126.

Kim, H. K., Choi, Y. H., & Verpoorte, R. (2011). NMR-based plant metabolomics: Where do we stand, where do we go? *Trends in Biotechnology, 29*, 267–275.

Kim, H. K., & Verpoorte, R. (2010). Sample preparation for plant metabolomics. *Phytochemical Analysis, 21*, 4–13.

Kinnersley, A. M., & Turano, F. J. (2000). Gamma aminobutyric acid (GABA) and plant responses to stress. *Critical Reviews in Plant Sciences, 19*, 479–509.

Kuzuyama, T., & Seto, H. (2003). Diversity of the biosynthesis of the isoprene units. *Natural Products Reports, 20*, 171–183.

Lian, M. L., Chakrabarty, D., & Paek, K. Y. (2002). Effect of plant growth regulators and medium composition on cell growth and saponin production during cell suspension culture of mountain ginseng (Panax ginseng C.A. Mayer). *Journal of Plant Biology, 45*, 201–206.

Manetti, C., Bianchetti, C., Bizzarri, M., Casciani, L., Castro, C., D'Ascenzo, G., et al. (2004). NMR-based metabonomic study of transgenic maize. *Phytochemistry, 65*, 3187–3198.

Manetti, C., Bianchetti, C., Casciani, L., Castro, C., Di Cocco, M. E., Miccheli, A., et al. (2006). A metabonomic study of transgenic maize (*Zea mays*) seeds revealed variations in osmolytes and branched amino acids. *Journal of Experimental Botany, 57*, 2613–2625.

Matsuda, F., Ishihara, A., Takanashi, K., Morino, K., Miyazawa, H., Wakasa, H., et al. (2010). Metabolic profiling analysis of genetically modified rice seedlings that overproduce tryptophan reveals the occurrence of its inter-tissue translocation. *Plant Biotechnology, 27*, 17–27.

Miccheli, A., Aureli, T., Delfini, M., Di Cocco, M. E., Viola, P., Gobetto, R., et al. (1988). Study on influence of inactivation enzyme techniques and extraction procedures on cerebral phosphorylated metabolite levels by 31P NMR spectroscopy. *Cellular and Molecular Biology, 34*, 591–603.

Modarai, M., Yang, M., Suter, A., Kortenkamp, A., & Heinrich, M. (2010). Metabolomic profiling of liquid Echinacea medicinal products with in vitro inhibitory effects on cytochrome P450 3A4 (CYP3A4). *Planta Medica, 76*, 378–385.

Motavalizadehkakhky, A. (2012). Antimicrobial activity and chemical composition of essential oils of four *Hypericum* from Khorasan, Iran. *Journal of Medicinal Plant Research, 6*, 2478–2487.

Nahrstedt, A., & Butterweck, V. (2010). Lessons learned from herbal medicinal products: The example of St. John's Wort (perpendicular). *Journal of Natural Products, 73*, 1015–1021.

Nürk, N. M., Madriñán, S., Carine, M. A., Chase, M. W., & Blattner, F. R. (2013). Molecular phylogenetics and morphological evolution of St. John's wort (*Hypericum*; Hypericaceae). *Molecular Phylogenetics and Evolution, 66*, 1–16.

Paek, K. Y., Murthy, H. N., Hahn, E. J., & Zhong, J. J. (2009). Large scale culture of ginseng adventitious roots for production of ginsenosides. *Advances in Biochemical Engineering/Biotechnology, 113*, 151–176.

Pasqua, G., Avato, P., Monacelli, B., Santamaria, A. R., & Argentieri, M. P. (2003). Metabolites in cell suspension cultures, calli, and in vitro regenerated organs of *Hypericum perforatum* cv. Topas. *Plant Science, 165*, 977–982.

Porzel, A., Farag, M. A., Mülbradt, J., & Wessjohann, L. A. (2013). Metabolite profiling and fingerprinting of *Hypericum* species: A

comparison of MS and NMR metabolomics. *Metabolomics*. doi:10.1007/s11306-013-0609-7.

Rao, S. R., & Ravishankar, G. A. (2002). Plant cell cultures: Chemical factories of secondary metabolites. *Biotechnology Advances, 20*, 101–153.

Rasmussen, B., Cloarec, O., Tang, H., Staerk, D., & Jaroszewski, J. W. (2006). Multivariate analysis of integrated and full-resolution ^{1}H-NMR spectral data from complex pharmaceutical preparations: St John's wort. *Planta Medica, 72*, 556–563.

Sacchettini, J. C., & Poulter, C. D. (1997). Creating isoprenoid diversity. *Science, 277*, 1788–1789.

Saddiqe, Z., Naeem, I., & Maimoona, A. (2010). A review of the antibacterial activity of *Hypericum perforatum*. *Journal of Ethnopharmacology, 131*, 511–521.

Sasse, J. M. (2003). Physiological actions of brassinosteroids: An update. *Journal of Plant Growth Regulation, 22*, 276–288.

Shelp, B. J., Bown, A. W., & McLean, M. D. (1999). Metabolism and functions of gamma-aminobutyric acid. *Trends in Plant Science, 4*, 446–452.

Sivanandhan, G., Arun, M., Mayavan, S., Rajesh, M., Mariashibu, T. S., Manickavasagam, M., et al. (2012). Chitosan enhances withanolides production in adventitious root cultures of *Withania somnifera* (L.) Dunal. *Industrial Crops and Products, 37*, 124–129.

Smilde, A. K., Jansen, J. J., Hoefsloot, H. C., Lamers, R. J., Van der Greef, J., & Timmerman, M. E. (2005). ANOVA-simultaneous component analysis (ASCA): A new tool for analyzing designed metabolomics data. *Bioinformatics, 21*, 3043–3048.

Snedden, W. A., Arazi, T., Fromm, H., & Shelp, B. J. (1995). Calcium/calmodulin activation of soybean glutamate decarboxylase. *Plant Physiology, 108*, 543–549.

Tocci, N., D'Auria, F. D., Simonetti, G., Panella, S., Palamara, A. T., Debrassi, A., et al. (2013). Bioassay-guided fractionation of extracts from *Hypericum perforatum in vitro* roots treated with carboxymethylchitosans and determination of antifungal activity against human fungal pathogens. *Plant Physiology and Biochemistry, 70*, 342–347.

Tocci, N., D'Auria, F. D., Simonetti, G., Panella, S., Palamara, A. T., & Pasqua, G. (2012). A three-step culture system to increase the xanthone production and antifungal activity of *Hypericum perforatum* subsp. *angustifolium in vitro* roots. *Plant Physiology and Biochemistry, 57*, 54–58.

Tocci, N., Simonetti, G., D'Auria, F. D., Panella, S., Palamara, A. T., Valletta, A., et al. (2011). Root cultures of *Hypericum perforatum* subsp. *angustifolium* elicited with chitosan and production of xanthone-rich extracts with antifungal activity. *Applied Microbiology and Biotechnology, 91*, 977–987.

Toyomasu, T., Kagahara, T., Okada, K., Koga, J., Hasegawa, M., Mitsuhashi, W., et al. (2008). Diterpene phytoalexins are biosynthesized in and exuded from the roots of rice seedlings. *Bioscience, Biotechnology, and Biochemistry, 72*, 562–567.

Vis, D. J., Westerhuis, J. A., Smilde, A. K., & Van der Greef, J. (2007). Statistical validation of megavariate effects in ASCA. *BMC Bioinformatics, 8*, 322.

Walker, T. S., Pal, Bais H., & Vivanco, J. M. (2002). Jasmonic acid-induced hypericin production in cell suspension cultures of *Hypericum perforatum* L. (St. John's wort). *Phytochemistry, 60*, 289–293.

Yaeno, T., Matsuda, O., & Iba, K. (2004). Role of chloroplast trienoic fatty acids in plant disease defense responses. *The Plant Journal, 40*, 931–941.

Yang, S. Y., Kim, H. K., Lefeber, A. W., Erkelens, C., Angelova, N., Choi, Y. H., et al. (2006). Application of two-dimensional nuclear magnetic resonance spectroscopy to quality control of ginseng commercial products. *Planta Medica, 72*, 364–369.

Yin, H., Fretté, X. C., Christensen, L. P., & Grevsen, K. (2012). Chitosan oligosaccharides promote the content of polyphenols in Greek oregano (*Origanum vulgare* ssp. *hirtum*). *Journal of Agriculture and Food Chemistry, 60*, 136–143.

Zhang, D. W., Liu, X., Xie, D., Chen, R., Tao, X. Y., Zou, J. H., et al. (2013). Two new diterpenoids from cell cultures of *Salvia miltiorrhiza*. *Chemical & Pharmaceutical Bulletin, 61*, 576–580.

Zhao, J., Davis, L. C., & Verpoorte, R. (2005). Elicitor signal transduction leading to production of plant secondary metabolites. *Biotechnology Advances, 23*, 283–333.

Zobayed, S. M. A., Murch, S. J., Rupasinghe, H. P. V., & Saxena, P. K. (2004). In vitro production and chemical characterization of St. John's wort (*Hypericum perforatum* L. cv 'New Stems'). *Plant Science, 166*, 333–340.

Zulak, K. G., Weljie, A. M., Vogel, H. J., & Facchini, P. J. (2008). Quantitative 1H NMR metabolomics reveals extensive metabolic reprogramming of primary and secondary metabolism in elicitor-treated opium poppy cell cultures. *BMC Plant Biology, 8*, 5.